

Study of the dependence of the degree of disordering of the surface layers of Si(111) and Ge(111) single crystals upon bombardment with low-energy ions

B.E. Umirzakov¹, I.R. Bekpulatov¹, G.T. Imanova^{*,2,3,4},
I.Kh. Turapov¹, J.M. Jumaev¹

¹Tashkent State Technical University, Tashkent, Uzbekistan

²Institute of Radiation Problems Ministry of Science and Education Republic of Azerbaijan, Baku, Azerbaijan

³UNEC Research Center for Sustainable Development and Green Economy named after Nizami Ganjavi, Baku, Azerbaijan

⁴Khazar University, Baku, Azerbaijan

E-mail: gunel_imanova55@mail.ru

DOI: [10.32523/ejpfm.2023070405](https://doi.org/10.32523/ejpfm.2023070405)

Received: 03.12.2023 - after revision

In the presented article, samples were studied using Auger electron spectroscopy, recording the angular dependences of the coefficient of elastically reflected electrons η , and spectroscopy of elastically reflected electrons. A change in the composition and degree of disorder of the surface layers of Si (111) was detected when bombarded with Ar^+ and K^+ ions with a change in energy $E_0 \sim$ from 1 to 10 keV and ion dose from $\sim 10^{13}$ to 10^{17} cm^{-2} . It was found that although the Ar and K atoms have the same masses, at the same ion energies, the degree of disordering of the near-surface Si(111) layer differs significantly. The observed effect is explained by the significant difference in their ionic radii. It is shown that at $E_0 \geq 3$ keV, the complete amorphization of near-surface layers occurs at relatively lower doses than surface amorphization.

Keywords: Si(111); Ge(111); single crystals; bombardment; low-energy; amorphization

Introduction

In recent years, the low-energy ion bombardment method has been widely used to obtain nanosized phases and films (layers) with desired physical properties on the surface of metals, semiconductors, and dielectric films [1–8]. In the process of ion bombardment of single crystals, along with a change in the composition of ion-doped layers, due to the formation of a large number of radiation defects, the surface layers are disordered up to amorphization. The latter leads to a significant change in the electronic structure, emission, optical and electrical properties of ion-implanted layers. At present, there is a large number of publications on the study of the dependence of the degree of disordering of the near-surface layers of single crystals on the dose and type of ions. These studies mainly refer to the implantation of high-energy ions ($E_0 \geq 20\text{--}30$ keV) [9, 10]. In the case of low-energy ions ($E_0 \leq 5\text{--}10$ keV), the results of studying the effect of ion implantation on their composition, electronic structure and properties are rather few devoted to the study of structures [11–21] and there are no reliable data.

In this work, we tried to study the effects of low-energy bombardment with Ar^+ and K^+ ions and subsequent annealing on the composition and crystal structure of ion-doped Si(111) layers.

Materials and Methods

The objects of study were well-polished single-crystal samples of p-type Si(111) (boron concentration $\sim 3 \cdot 10^{18} \text{ cm}^{-3}$) with dimensions of $10 \times 10 \times 0.3$ mm. All technological treatments (heating, bombardment with Ar^+ and K^+ ions) and studies of the composition, structure using Auger electron spectroscopy (AES), registration of the angular dependences of the coefficient of inelastically reflected electrons (CIRE) $\eta(\varphi)$ and the dependence of dR/dE_p on dE_p spectroscopy of elastically reflected slow electrons (SERSE) were carried out in the same device (USU-2 type) in vacuum $P \leq 10^{-7}$ Pa. In this relation R is the coefficient of elastically reflected electrons, E_p is the energy of primary electrons. The energy of Ar^+ and K^+ ions varied within $E_0 = 1\text{--}10$ keV, and their dose was from $10^{13}\text{--}10^{17} \text{ cm}^{-2}$. Before ion bombardment, the Si surface was degassed at $T \approx 1150$ K for 4–5 hours in combination with short-term heating to $T = 1300$ K. The depth distribution profiles of potassium atoms were determined by the AES method in combination with etching of the Si surface with Ar^+ ions with $E_0 \approx 1.5$ keV at an angle of $10\text{--}15^\circ$ relative to the surface.

Since at low ion energies the thickness d of disordered layers is only $100\text{--}150$ Å, the methods of recording $\eta(\varphi)$ and dR/dE_p (dE_p) were used to estimate the degree of disorder.

The $\eta(\varphi)$ curves were recorded at an energy of primary electrons $E_p = 600$ eV. In this case, the depth of the SERSE exit d_η at $\varphi = 0$ for Si, calculated by the Bronstein formula [22]: $d_e = L_e/2 = 3 \cdot 10^{-6} \text{ AEP}^{1.4}/\rho Z$ is $\sim 80\text{--}100$ Å, which completely covers the ion bombarded Si layers. At $\varphi \approx 50\text{--}60^\circ$, the value of d_η fits in ~ 1.5 times. Here L_e is the depth of penetration of primary electrons

in cm, ρ is the density in g/cm^3 ; A – is the atomic weight, Z – is the ordinal number of the element.

Dependence $\eta(\varphi)$ gives exhaustive information about the degree of disordering of near-surface layers of single crystals up to a thickness of 100–120 Å, and SERSE gives information about surface layers ~ 2 –3 monolayers thick.

Results and discussion

The study of the effect of ion bombardment on the composition, structure and properties of even elementary semiconductors is associated with great difficulties, in particular, ion bombardment is accompanied by the decomposition of covalent bonds between atoms, disorder due to the appearance of radiation defects and dislocations in ion-implanted layers, the formation of new compounds, diffusion and desorption of atoms, and annealing of radiation defects can also occur. These changes depend on the energy, dose and type of bombarding ions. In this work, the main attention was paid to the change in the crystal structure of Si(111) during ion bombardment and subsequent annealing. To exclude defect annealing, bombardment was carried out at low current densities: $J \leq 0.5 \mu\text{A}/\text{cm}^2$. Figure 1 shows the angular dependences $\eta(\varphi)$ for Si bombarded with Ar^+ ions with $E_0 = 5 \text{ keV}$ at different irradiation doses D . Here η_{600} is the value of the electron inelastic reflection coefficient at $E_p = 600 \text{ eV}$.

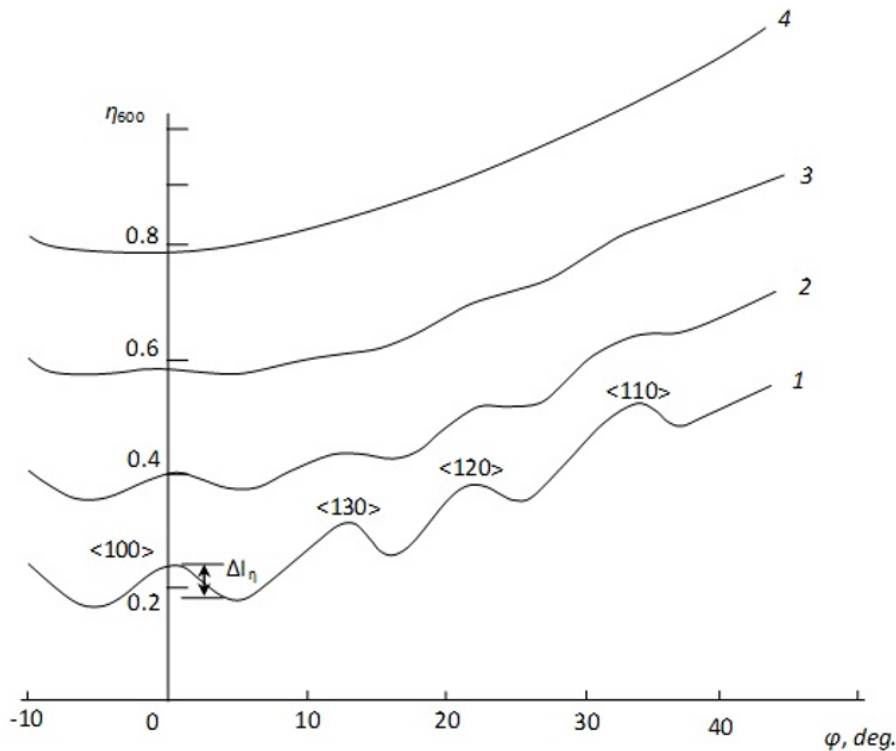


Figure 1. Angular dependences $\eta(\varphi)$ for Si bombarded with Ar^+ ions with $E_0 = 5 \text{ keV}$ at different doses D , cm^{-2} : 1 – 0; 2 – $6 \cdot 10^{13}$; 3 – $2 \cdot 10^{14}$; 4 – $2 \cdot 10^{15}$.

It can be seen that the dependence $\eta(\varphi)$ of pure Si samples pronounced maxima corresponding to different crystal directions of Si(111). In the case of

ion bombardment with low doses, the intensity of all maxima decreases. In this case, the peak intensities at angles less than $\sim 20\text{--}30^\circ$ fit faster. Already at $D \approx 2 \cdot 10^{14} \text{ cm}^{-2}$, all the maxima are practically smoothed out, i.e. complete disordering of the near-surface Si layers occurs.

Figure 2 shows the dependence of the intensity of the first maximum, ΔI_η , on the irradiation dose for Si(111) bombarded by Ar^+ and K^+ ions with $E_0 = 3 \text{ keV}$ at different doses. Dependences, regardless of the type of ion, show three characteristic areas: at low doses, ΔI_η decreases slightly, then there is a sharp decrease, and starting from a certain dose, the value of ΔI_η approaches zero, i.e. there is a complete disordering (amorphization) of ion-bombarded layers. In the case of Ar^+ ions, disordering starts from $D \approx 2 \cdot 10^{14} \text{ cm}^{-2}$, and complete amorphization occurs from $D \approx 6 \cdot 10^{14} \text{ cm}^{-2}$. In the case of Na^+ , disordering starts from $D \approx 5 \cdot 10^{14} \text{ cm}^{-2}$, and complete amorphization from $2 \cdot 10^{15} \text{ cm}^{-2}$. The masses and atomic radii of Ar^+ and K^+ differ little from each other. Therefore, the observed differences in the degree of amorphization can be explained by a sharp difference in their ionic radii: $r_{\text{Ar}^+} \approx 1.88 \text{ \AA}$, $r_{\text{K}^+} \approx 1.33 \text{ \AA}$.

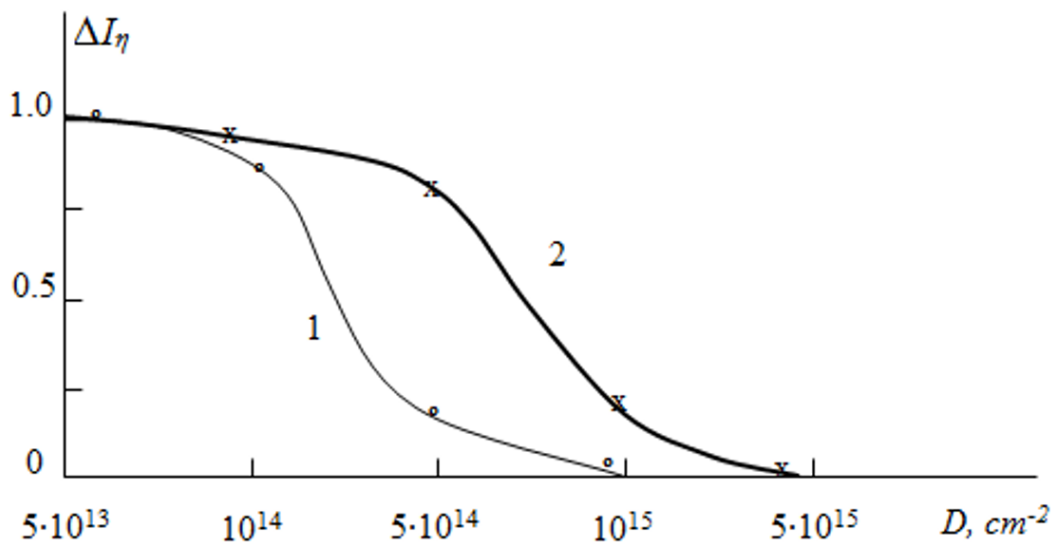


Figure 2. Dependence of the relative intensity of the main maximum of silicon ΔI_η on the irradiation dose at $E_0 = 3 \text{ keV}$: 1 – Ar^+ ; 2 – K^+ .

The degree of amorphization depends on the energy of the ions. Figure 3 shows the dependence of ΔI_η on the radiation dose for Si(111) bombarded with Ar^+ ions with $E_0 = 1, 3,$ and 10 keV .

It can be seen from Figure 3 that at $E_0 = 1 \text{ keV}$ the disordering occurs slowly and the characteristic regions are not sharply distinguished. In the case of $E_0 = 10 \text{ keV}$, the characteristic regions are very similar for $E_0 = 3 \text{ keV}$ and slightly shift towards lower doses. Apparently, at low ion energies, the relative number of breaking bonds between Si atoms is much less than in the case of $E_0 \geq 3 \text{ keV}$. Note that at $E_0 > 10 \text{ keV}$, as E_0 increases, the behavior of the curves $\Delta I_\eta(D)$ and the degree of amorphization of Si change insignificantly.

It is known that the dependences of dR/dE_p on E_p spectra elastically reflected electrons (SERE) in the region of $E_p \approx 30\text{--}200 \text{ eV}$, along with the peaks characteristic of interband transitions, show well features associated with diffrac-

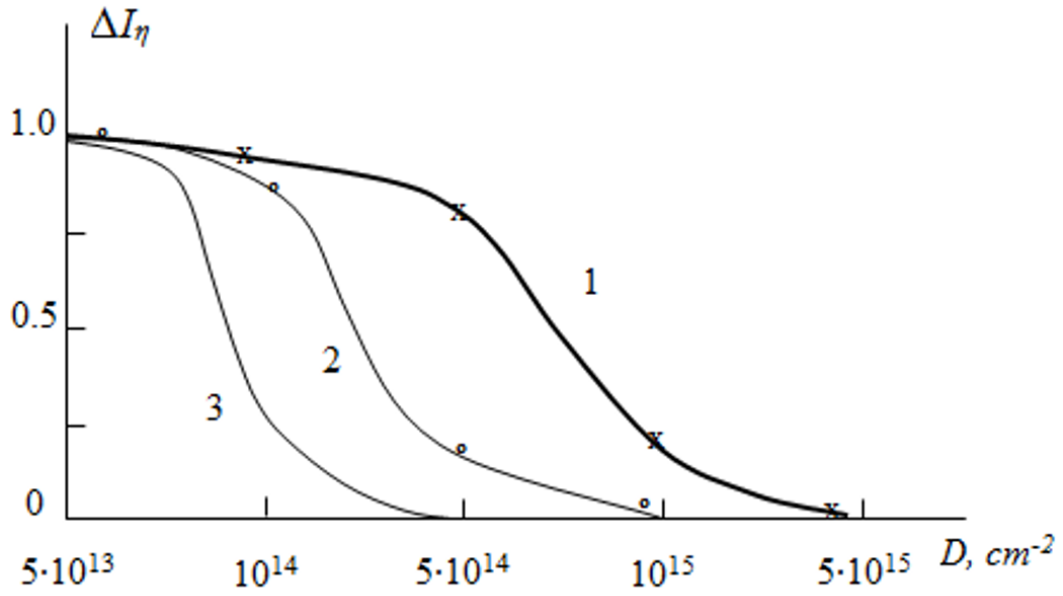


Figure 3. Dependence $\Delta I_{\eta}(D)$ for Si(111) bombarded with Ar^+ ions with E_0 : 1–1 keV; 2–3 keV; and 3–10 keV.

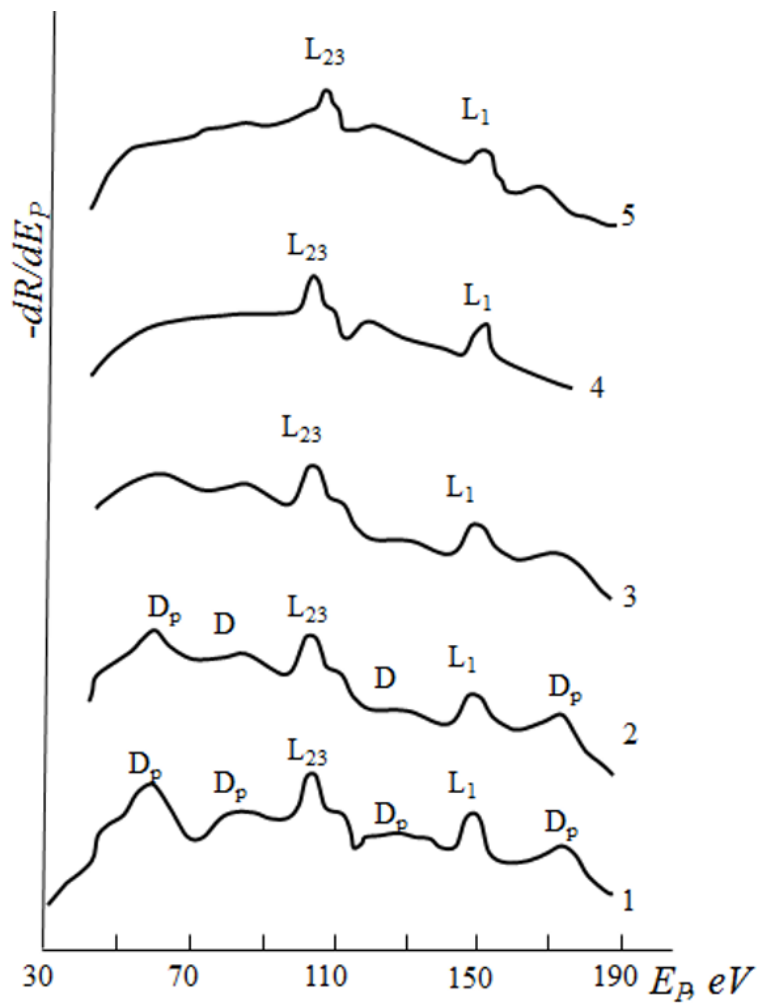


Figure 4. SERSE spectra of Ge(111) bombarded with Ar^+ ions with $E_0 = 3$ keV at doses D, cm^{-2} : 1 – 0; 2 – $2 \cdot 10^{14}$; 3 – $8 \cdot 10^{14}$; 4 – $2 \cdot 10^{15}$, 5 – $6 \cdot 10^{15}$.

tion phenomena. Figure 4 shows the dependences of dR/dE_p (E_p) for Ge(111)

bombarded with Ar^+ ions with $E_0=3$ keV at different doses. It can be seen that the intensity of the diffraction peaks D_p decreases with increasing D , while the intensity of the peaks of interband transitions does not noticeably change. Apparently, during the bombardment, the composition of the ion-bombarded layers does not noticeably change, only disordering occurs. Curve 2 shows that the diffraction peaks do not disappear up to a dose of $8 \cdot 10^{14} \text{ cm}^{-2}$. In the case of $\eta(\varphi)$, the diffraction maxima are completely smoothed out at $D=5 \cdot 10^{14} \text{ cm}^{-2}$. Apparently, due to the uneven distribution of defects, in cases of $E_0 \geq 5$ keV, amorphization begins from the depths of the projected path [23, 24]. Note that at $E_0 \leq 1\text{--}2$ keV, the diffraction peaks in the dependences dR/dE_p (E_p) and $\eta(\varphi)$ are completely smoothed out at approximately the same doses. At these energies E_0 , the R_p value is very close to the surface and amounts to $\approx 20\text{--}30 \text{ \AA}$.

Conclusion

It is shown that, at the same ion energies, the complete disordering of the near-surface layers of single-crystal Si(111) in the case of Ar^+ ions occurs at lower doses than in the case of Na^+ ions. The difference in the degree of amorphization is related to the difference between the ionic radii of Ar^+ and K^+ .

The dependence of the degree of amorphization on the ion energy is determined. At low ion energies ($E_0 \approx 1$ keV), amorphization begins at relatively higher doses than at $E_0 \geq 3$ keV.

It is shown that, at $E_0 \geq 5$ keV, the disordering of the Si(111) layers starts from the depth of the projected range. Therefore, for example, in the case of Ar^+ ions with $E_0=5$ keV, although the complete disordering of the near-surface layers occurs at $6 \cdot 10^{14} \text{ cm}^{-2}$, and the surface is disordered only at $\sim 2 \cdot 10^{15} \text{ cm}^{-2}$. At low ion energies ($E_0=1$ keV), due to the small value of R_p , the surface and near-surface region of Si(111) are disordered almost simultaneously.

References

- [1] W. Jiang et al., Phys. Rev. B **80** (2009) 161301(R). [[CrossRef](#)]
- [2] W.L. Chan, E. Chason, J. Appl. Phys. **101** (2007) 121301. [[CrossRef](#)]
- [3] D. Gupta et al., Scientific Reports **9** (2019) 15531. [[CrossRef](#)]
- [4] P.A. Bennett et al., Applied Surface Science **180** (2001) 65–72. [[CrossRef](#)]
- [5] R. Ayache et al., International Journal of Thin Films Science and Technology **4** (2015) 211–213. [[CrossRef](#)]
- [6] Sh. Zhou et al., Phys. Rev. B **75** (2007) 085203. [[CrossRef](#)]
- [7] Y.S. Ergashov, B.E. Umirzakov, Journal of Surface Investigation: X-ray, Synchrotron and Neutron Techniques **12** (2018) 816–818. [[CrossRef](#)]
- [8] S.B. Donaev et al., Technical Physics **64** (2019) 1541–1543. [[CrossRef](#)]
- [9] G.A. Schiffrin, R.G. Hunsperger, Appl. Phys. Letters **17** (1970) 274–276. [[CrossRef](#)]
- [10] G.T. Imanova, Advanced Physical Research **2** (2020) 94–101. [[WebLink](#)]

- [11] S.B. Donaev et al., IOP Conference Series: Earth and Environmental Science **614** (2020) 012002. [[CrossRef](#)]
- [12] I.Kh. Turapov et al., Technical Physics Letters **48** (2022) 25–27. [[CrossRef](#)]
- [13] B.E. Umirzakov et al., Journal of Surface Investigation: X-ray, Synchrotron and Neutron Techniques **17** (2023) 317–320. [[CrossRef](#)]
- [14] I. Bekpulatov et al., International Scientific Conference on Construction Mechanics, Hydraulics and Water Resources Engineering, Conmechhydro (2021) Tashkent **264** (2021) 05037. [[CrossRef](#)]
- [15] B.E. Umirzakov et al., Modern Physics Letters B **37** (2023) 2350078. [[CrossRef](#)]
- [16] M.T. Normuradov et al., Advanced Physical Research **4** (2022) 142–154. [[WebLink](#)]
- [17] B.E. Umirzakov, S.B. Donaev, Journal of Surface Investigation: X-ray, Synchrotron and Neutron Techniques **11** (2017) 746–748. [[CrossRef](#)]
- [18] H.I. Lee et al., Nuclear Instruments and Methods in Physics Research Section B: Beam Interactions with Materials and Atoms **219–220** (2004) 959–962. [[CrossRef](#)]
- [19] P.M. Gevers et al., J. Vac. Sci. Technol. A **28** (2010) 293–301. [[CrossRef](#)]
- [20] W.M. Lau et al., J. Appl. Phys. **75** (1994) 3385–3391. [[CrossRef](#)]
- [21] D. Humbird et al., Journal of Vacuum Science and Technology A **25** (2007) 1529–1533. [[CrossRef](#)]
- [22] I.M. Bronstein, B.S. Fryman, Secondary electron emission (M.: Science, 1969) 407 p. (In Russian)
- [23] P. Kumar, Semiconductor Science and Technology **31** (2016) 035014. [[CrossRef](#)]
- [24] I.R. Bekpulatov et al., International Journal of Modern Physics B **37** (2023) 22350164. [[CrossRef](#)]